Biogeosciences, 22, 6963–6978, 2025 https://doi.org/10.5194/bg-22-6963-2025 © Author(s) 2025. This work is distributed under the Creative Commons Attribution 4.0 License.





Modeling the mechanisms of coastal vegetation dynamics and ecosystem responses to changing water levels

Junyan Ding¹, Nate McDowell^{2,3}, Vanessa Bailey², Nate Conroy⁴, Donnie J. Day⁵, Yilin Fang⁶, Kenneth M. Kemner⁷, Matthew L. Kirwan⁸, Charlie D. Koven⁹, Matthew Kovach⁵, Patrick Megonigal¹⁰, Kendalynn A. Morris¹¹, Teri O'Meara¹², Stephanie C. Pennington¹¹, Roberta B. Peixoto⁵, Peter Thornton¹², Mike Weintraub⁵, Peter Regier¹³, Leticia Sandoval⁵, Fausto Machado-Silva⁵, Alice Stearns¹⁰, Nick Ward¹³, and Stephanie J. Wilson¹⁰

Correspondence: Junyan Ding (jding@oxy.edu)

Received: 3 April 2025 – Discussion started: 25 April 2025

Revised: 1 October 2025 - Accepted: 14 October 2025 - Published: 20 November 2025

Abstract. Coastal forests are increasingly experiencing mortality due to inundation by fresh- and seawater, leading to their replacement by marshes. These shifts alter vegetation composition, biogeochemical cycling, carbon storage, and hydrology. Using a hydraulically enabled ecosystem demography model (FATES-Hydro), we conducted numerical experiments to investigate the mechanisms behind inundation-driven forest loss and the ecosystem-scale consequences of forest-to-marsh transitions. We compared mortality processes and their effects across broadleaf and conifer trees at two coastal sites – Lake Erie (freshwater) and Chesapeake Bay (saline).

Our simulations show that hydraulic failure, driven by root loss under prolonged flooding, is the primary mortality mechanism across both tree types and sites. Forest replacement by marsh reduced ecosystem-scale leaf area index (LAI), gross primary production (GPP), transpiration, and deep soil water uptake in conifer forests, while broadleaf

forests experienced smaller changes due to lower initial LAI and greater marsh compensation. Marsh invasion occurred following canopy thinning driven by tree mortality. These findings suggest that, under similar root loss, hydraulic failure dominates coastal tree mortality regardless of species or water type, with denser forests experiencing stronger ecosystem impacts. Our study identifies key mortality mechanisms and offers testable hypotheses for future empirical studies on coastal vegetation change.

1 Introduction

Shoreline vegetation provides important ecosystem functions (Barbier et al., 2011; Mitsch et al., 2015). Coastal forests can be more productive than adjacent upland systems (Tagestad et al., 2021), have larger carbon stocks than the marshes replacing them (Smith et al., 2021), mitigate storm-driven ero-

¹Department of Biology, Occidental College, Los Angeles, CA 90041, USA

²Biological Science Division, Pacific Northwest National Laboratory, Richland, WA 99352, USA

³School of Biological Sciences, Washington State University, P.O. Box 644236, Pullman, WA 99164-4236, USA

⁴Earth and Environmental Sciences Division, Los Alamos National Laboratory, Los Alamos, New Mexico 87545, USA

⁵The University of Toledo, Toledo, OH 43606, USA

⁶Earth Systems Science Division, Pacific Northwest National Laboratory, Richland, WA 99352, USA

⁷Molecular Environmental Sciences Group, Argonne National Laboratory, Lemont, IL 60439, USA

⁸Virginia Institute of Marine Science, College of William and Mary, Gloucester Point, VA 23062, USA

⁹Climate and Ecosystem Sciences Division, Lawrence Berkeley National Laboratory, Berkeley, CA 94720, USA

¹⁰Smithsonian Environmental Research Center, Edgewater, MD 21037, USA

¹¹Joint Global Change Research Institute, Pacific Northwest National Laboratory, College Park, MD 20740, USA

¹²Environmental Sciences Division, Oak Ridge National Laboratory, Oak Ridge, TN 37830, USA

¹³Marine and Coastal Research Laboratory, Pacific Northwest National Laboratory, Sequim, WA 98382, USA

sion (Arkema et al., 2013; Spalding et al., 2014), and provide habitat for a wide variety of animals (Duarte et al., 2013; Barbier, 2013; Mitsch et al., 2015). Coastal ecosystems are experiencing rapid increases in tree mortality due to changing water levels in both fresh- and seawater systems (Mc-Dowell et al., 2022). Globally, sea-level rise and flooding threaten coastal forests, with potential habitat losses ranging from less than 10 % with a 1 m rise to as much as 55 % under a 3 m rise scenario (Ury et al., 2021). Increasingly variable freshwater levels in lakes and accelerating sea level rise (SLR) are anticipated with climate change (Varekamp et al., 1992; Mimura, 2013; Theuerkauf et al., 2019; Kayastha et al., 2022; Saber et al., 2023). Varying water levels induce large changes in species composition, including shifts from forest to marsh, driven in part by tree mortality (Keddy and Reznicek, 1986; Hudon, 1997; Frieswyk and Zedler, 2007; Wilcox, 2004; Wilcox and Nichols, 2008).

Soil hypoxia and salinity are key drivers of tree mortality under increasing inundation. Prolonged increases in hypoxia and soil salinity reduce root hydraulic conductance and promote root loss (Colmer and Flowers, 2008; Pezeshki et al., 1987). Elevated soil salinity also reduces soil water potential (Boursiac et al., 2005), thereby reducing the soilto-root water potential gradient that drives water movement into roots. Together, these belowground impacts of rising hypoxia and salinity reduce whole-plant hydraulic conductivity (López-Berenguer et al., 2006; Nedjimi, 2014), subsequently increasing the likelihood of xylem embolism and mortality from hydraulic failure (McDowell et al., 2022). These reductions in whole-plant conductivity can promote carbon starvation through declining stomatal conductance (Orsini et al., 2012; Sperry et al., 2016) and leaf loss (Munns and Termaat, 1986; Wang et al., 2019; Zhang et al., 2021b). Increased salt concentrations inhibit potassium accumulation in guard cells, also promoting stomatal closure (Clough and Simm, 1989; Perri et al., 2019). These photosynthetic constraints can be exacerbated by foliar ion toxicity that impairs photosynthetic biochemistry (Ball and Farquhar, 1984; Delatorre-Herrera et al., 2021; Munns, 2005; Suárez and Medina, 2006; Li et al., 2021; Yadav et al., 2011).

Physiological impacts from hypoxia and salinity can also vary with the frequency and duration of inundation and with interspecific variation in physiological traits. Freshwater systems experience variable inundation across seasons and years (Fig. 1) and may have opportunity to recover from inundation, whereas SLR induces a chronic rise in inundation that can reduce recovery (Taherkhani et al., 2020; Thiéblemont et al., 2023). Interspecific trait differences such as in xylem vulnerability to cavitation can also influence the degree of mortality (Niknam and McComb, 2000; Sairam et al., 2008; Acosta-Motos et al., 2017; Zhao et al., 2020; McDowell et al., 2022). Mortality mechanism tests have not addressed inundation dynamics and interspecific variation.

Coastal tree mortality has large impacts on ecosystem function (Kirwan and Gedan, 2019). Tree mortality reduces

forest biomass and leaf area (Chen and Kirwan, 2022b), which in turn provides a light environment favorable for the expansion of marsh vegetation (Shaw et al., 2022; Sward et al., 2023). This results in transpiration and carbon uptake and storage shifting from trees to marsh plants as forests retreat, with net reductions in fluxes and storage depending on the degree of compensation by the invading marsh (Smith et al., 2021; Davidson et al., 2018; Zhou et al., 2023). However, the effects of tree death and marsh invasion on ecosystem-scale fluxes and their underlying mechanisms are poorly known (Kirwan et al., 2024).

In a recent study, Ding et al. (2023b) incorporated the effects of salinity and hypoxia on root loss, hydraulic function, and photosynthesis into the process-based ecosystem demographic model FATES-Hydro to simulate physiological responses of conifer trees to seawater exposure. They applied the model to three coastal conifer forests in the US, finding that both hydraulic failure and carbon starvation contribute to tree mortality, with the dominant mechanism depending on the rate and duration of salinization. Rapid exposure favored carbon starvation, while chronic inundation led primarily to hydraulic failure.

Building upon Ding et al. (2023b), which focuses on physiological responses of conifer trees to seawater exposure, here we extend the investigation to broadleaf deciduous trees, allowing evaluation of how functional traits such as photosynthetic capacity, morphology, and phenology influence mortality outcomes under similar belowground stress conditions. Because the two tree types have very different physiology, morphology and phenology, we specifically examine to which extent the difference in these traits can affect the response of trees to hypoxia and salinity if root loss are the same. We also incorporate a freshwater coastal system (Lake Erie) alongside a saline coastal site to compare how hydrologic context shapes vegetation transitions. We further assess ecosystem-scale consequences of tree mortality, including its impact on vegetation composition, and ecosystem fluxes. We conducted numerical experiments using Ding et al. (2023b) FATES-Hydro with a reciprocal design where the two tree types were simulated for both the freshwater and saline coasts to partition the role of species from their environment. We expect the broadleaf deciduous trees will be more susceptible to carbon starvation particular at saline coastal than conifers.

2 Methods

2.1 Study areas

The first site is located on the south shore of Lake Erie (the LE site) in Ohio, USA (41.48° N, 83.06° W) (Fig. S1 in the Supplement). The area has warm and humid summers and cold winters. The LE site is dominated by the broadleaf species shellbark hickory (*Carya laciniosa*) and

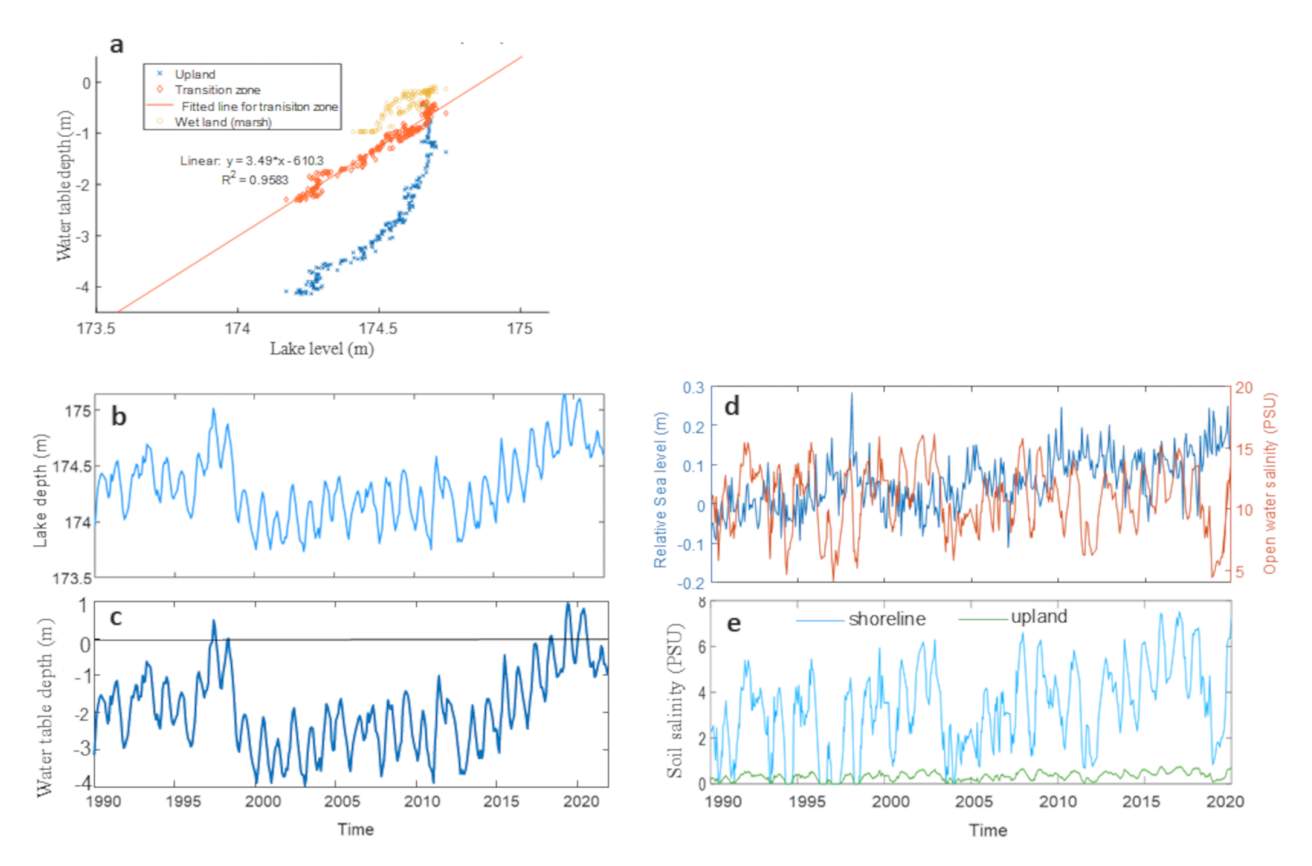


Figure 1. Study area: (a) relation between lake depth and soil water table depth in 2022, at the Lake Erie site transition zone corresponding to the shoreline location in simulations; (b) depth of Lake Erie 1990–2020; (c) Estimated water table depth at Lake Erie (LE) shoreline location; (d) sea level and open water salinity of the nearby station of Chesapeake Bay (CPB); and (e) Estimated soil salinity at CPB site

swamp white oak (*Quercus bicolor*). Lake Erie is part of the Great Lakes of North America, a series of interconnected large freshwater lakes. The water level of Lake Erie is subject to daily, seasonal, interannual, and decadal variation resulting from the complex interactions between climate, bathymetry, and the water levels of the upper lakes (Burlakova et al., 2014). Increases in the water levels in Lake Erie have resulted in extensive coastal tree mortality (Sippo et al., 2018; Theuerkauf and Braun, 2021).

The second site is located on the Chesapeake Bay (CB) in Maryland, USA (38.5° N, 76.3° W; Smith and Kirwan, 2021) (Fig. S1). The CB site is dominated by coniferous loblolly pine (*Pinus taeda*) forests, and the climate is characterized by warm, humid summers and cool winters. The CB region is a hotspot for sea-level driven coastal forest retreat, driven in part by the extensive low lying coastal plain topography (Schieder et al., 2018; Chen and Kirwan, 2022b). In the 21st century, relative SLR rates in the CB region (~3 to 6 mm yr⁻¹) are approximately two to three times faster than the global average (Sallenger et al., 2012; Ezer and Corlett, 2012).

In 2022, two forested study plots were established within the dying shoreline forests and in the neighboring unflooded uplands at each site. Stand level measurements include tree density, diameter at breast height (DBH) and water table depth. Tree-specific measurements were taken from eight live trees in each plot, which included growth, non-structural carbohydrates, continues hourly sap flow, leaf gas exchange, leaf photosynthetic capacity, and hourly leaf water potential (LWP) including predawn and mid-day LWP of a given day during the growing season. These eight live trees were bored to obtain tree cores for measurements of ring width growth along with eight dead trees located at the shoreline. We follow exactly the same measurements and sample processing as described in Zhang et al. (2021a), Wang et al. (2022). Here, we benchmarked the FATES-Hydro model against empirical data collected at each site.

2.2 Numerical experiments with the FATES-Hydro model

We conducted numerical experiments at both the LE and CB sites using a newly developed version of the ecosystem demography model, FATES-Hydro (Ding et al., 2023b), which represents the physiological impacts of hypoxia and salinity on plants and consequent changes in root conductance and mortality. All simulations were run with FATES-Hydro within the E3SM Land Model (ELM). Here we describe this

version of FATES-Hydro, its parameterization and benchmarking for this study, and the design of the numerical experiments.

2.2.1 Description of FATES-Hydro

The Functionally Assembled Terrestrial Ecosystem Simulator (FATES) is a physiology-based vegetation demographic model that simulates cohort-scale dynamics for different plant functional types (PFTs) (Fisher et al., 2018; Koven et al., 2020). FATES-Hydro is a version that integrates the plant hydraulics and their coupling with photosynthesis (Ding et al., 2023a). In FATES-Hydro plant transpiration is the product of whole-plant leaf area and the transpiration rate per unit leaf area (J), which itself is the product of stomatal conductance and vapor pressure difference from leaf intercellular spaces to bulk atmosphere. The hydro-dynamic module represents a plant's roots, xylem, and foliage as a variably porous media (Sperry et al., 1998) with conductance and capacitance changing in response to tissue water potentials dictated by the pressure-volume (P-V) curve and the pressure-conductance (vulnerability) curve (Manzoni, 2014; Christoffersen et al., 2016). Stomatal conductance is modified from the Ball-Berry model (Ball et al., 1984; Oleson et al., 2013; Fisher et al., 2015) with a further constraint of leaf water potential through a water stress index βt , defined by a function of the ratio of the leaf water potential to the leaf water potential of half stomatal closure (P50gs) (Christoffersen et al., 2016). The soil column is divided into 20 layers. The proportion of roots in each layer is calculated from Zeng's (2001) two parameter power law function. Water flow from each soil layer within the root zone into the plant root system is calculated as a function of the hydraulic conductance determined by root biomass and root traits such as specific root length, and the difference in water potential between the absorbing roots and the rhizosphere, and the transpiration is the sum of root water uptake from all soil layers. Additional technical details and parameter sensitivity analysis can be found in the technical notes (FATES Development Team, 2023, https://fates-users-guide.readthedocs. io/projects/tech-doc/en/latest/index.html, last access: 13 November 2013) and publications (e.g. Koven et al., 2020; Xu et al., 2023; Ding et al., 2023a, b; Robbins et al., 2024).

The version of FATES-Hydro used in this study also includes representation of the mechanisms by which soil hypoxia and salinity impact tree physiology and mortality (Ding et al., 2023b). The complete description of these new developments can be found in Ding et al. (2023b). Below we describe the root loss function because this is the key component in this study.

The root loss function (kr_{red}), expressed as the proportion of the root conductance under normal condition, is composed of hypoxia reduction ($kr_{red,sat}$) and the salinity reduction ($kr_{red,sal}$), expressed as:

$$kr_{red} = kr_{red,sat} \cdot kr_{red,sal} \tag{1}$$

Each term varies between near zero to 1, with near zero means no roots and 1 means the roots grow as normal.

The hypoxia reduction ratio is given as:

$$kr_{\text{red,sat}} = \frac{1}{1 + h \cdot e^{ks(x - x_0)}} \tag{2}$$

where b and ks are the scaling parameters that determine the rate of fine root loss from saturation; x (hours) is the total duration of the volumetric soil water content [m³ m⁻³] exceeds 90% saturation over a defined previous period of x_0 . Biologically, parameter b and ks can be used to represent how well the root system of the trees are adapted to waterlogging condition (Fig. S2).

The salinity reduction ratio is given by a salinity cumulation term (acc_sal) as:

$$kr_{red,sal} = exp(-kc \times acc_{sal})$$
 (3a)

$$acc_{sal} = max \left[\sum (Sal_{soil,t} - Sal_{cr}) \right]$$
 (3b)

where kc is a parameter determining the rate of fine root loss due to salinity, and acc_{sal} represents the cumulative salinity stress, calculated by summing the difference between soil salinity $(Sal_{soil,t})$ and a critical threshold (Sal_{cr}) beyond which salinity starts to negatively affect root mass, over all timesteps (i) up to the current step n. All terms are in PSU. As this formulation is dependent on the model's timestep, all simulations were run with a fixed temporal resolution of 30 min.

2.2.2 Parameterization and benchmarking

For the pine and the salinity induced root loss rate, the parameters used in Ding et al. (2025) were used in this study. For the broadleaf trees at Lake Erie, the parameters used in FATES-Hydro were either from field observations or obtained from the TRY trait database (Kattge et al., 2020) when field observation were not available (Table S1 in the Supplement). $V_{\rm cmax}$ was estimated from A/Ci curves and then adjusted within the observed range so that the simulated hourly $A_{\rm net}$ matched the fitted line of observed values (Fig. S2). P50_{gs} was adjusted within the ranges of the temperate broadleaf trees from the TRY database so that the simulated hourly leaf water potential matches the fitting curved based on measured hourly LWP (Fig. S2).

The allometry parameters that define the relationships between diameter at breast height and total tree height, sapwood area, total woody biomass, and total leaf biomass were estimated based on values of the Biomass and Allometry Database (BAAD) (Falster et al., 2015). The complete

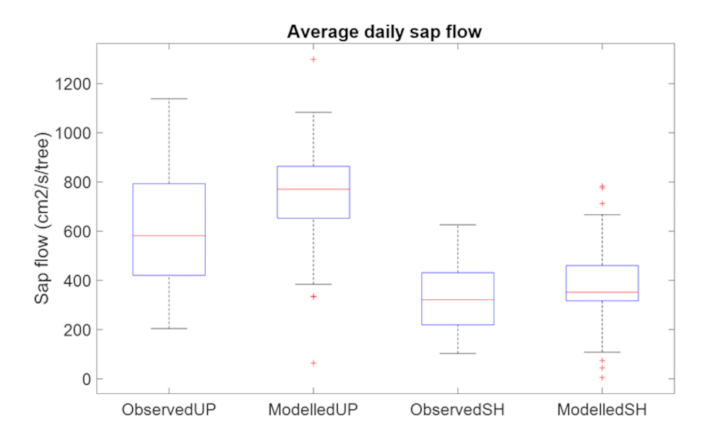


Figure 2. Benchmark root loss function by comparing measured and simulated average daily sap flow of August and September 2022 at upland location and shoreline location at LE site.

list of parameters can be found in the GitHub repository: https://github.com/JunyanDing/FATES_COMPASS (last access: 14 November 2025).

To calibrate the plant hydraulic parameters, K_{max} and xylem vulnerability curves, we first adjusted the parameters within the observed range of values for our broadleaf species (Kattge et al., 2020) from TRY database of the site to be close to measured hourly values and then we adjusted the phenology parameters so that the decline of simulated sap flow matched the observed pattern (Fig. S4 top panel). For saturation induced root loss function, based on previous studies (Islam and Macdonald, 2004; Aroca et al., 2012; Karlova et al., 2021) and unpublished experimental observations (Brennan et al., 2025), we set x_0 to 120 h (5 d) for this study. We then adjusted the root loss parameter ks so simulated sap flow was close to the mean of the observed values (Fig. S4 bottom panel) at the shoreline location with observed water table depth. The simulated average daily sap flow at upland and shoreline locations matches well with observations (Fig. 2). While perfect agreement is not expected, we find that the model reasonably captures the seasonal pattern and interannual variability of sap flow.

For the marsh grass, we use the biochemical and physiological parameters from O'Meara et al. (2021) and the allometry (height and total leaf area to stem width ratio) was estimated based on GCReW data (https://serc.si.edu/gcrew/data, last access: 14 November 2025). Because marsh plants are annual or bi-annual, phenology and maximum density (number of individuals per ground area), which control the variation of total leaf area, play a more important role in marsh ecosystems than plant physiology. We specifically calibrated these parameters. The phenology parameters are estimated based on the NDVI values from Chen and Kirwan (2022a) and the 2022 field measurement of sap flow at the LE upland site. The phenology parameters are same for both marsh plants and broadleaf trees, meaning marsh plant and broadleaf trees have same leaf on and off times. The NDVI

values at the neighboring wetlands indicate the marsh grass system had an LAI $\sim 2\,(\text{m}^2\,\text{m}^{-2})$ during the peak growing season. We further constrained the maximum density of the marsh to a growing season LAI of 2 $\text{m}^2\,\text{m}^{-2}$. To calibrate the broadleaf trees, we ran the model at LE site in 2022 initialized by the inventory data, then compared the model output with the field observations of photosynthesis, leaf water potential (Fig. S2), and sap flow (Fig. S3). We confirmed that the simulated growth rates over the 30-year simulation period fell within the observed range of tree ring widths measured from tree cores (Fig. S5). Note, our goal was to assess if simulated growth rates were within the range of observations to enable hypothesis tests, not to reproduce observed interannual growth variability at the individual tree level.

2.2.3 Setup of numerical experiments

The numerical experiments involved three plant functional types (PFT): broadleaf deciduous tree, evergreen conifer tree, and herbaceous marsh plants. We will call them broadleaf tree, conifer tree, and marsh plants hereafter. Each simulation was constructed either as broadleaf tree-marsh or as conifer tree-marsh combination. We first simulated the LE site using its native vegetation, the broadleaf trees and marsh, and the CB site using its native vegetation, conifer trees, and marsh. We then swapped the tree types between sites, such that the broadleaf forest was simulated at CB and the conifer forest at LE. The simulations of virtual forests at each site allowed investigation of how different forest types may respond to the differing drivers, i.e., with and without salinity. For both experiments we also examined the ecosystem-scale consequences of forest loss, namely on total evapotranspiration and photosynthetic carbon fluxes.

The simulations were driven by the University of East Anglia Climatic Research Unit (CRU) Japanese Reanalysis (JRA) meteorological product (CRUJRA) (University of East Anglia Climatic Research Unit; Harris, 2019) for 1990 through 2019. The simulations were initialized with inventory data of upland locations for the trees at both sites (Fig. S1). We used the observed inventory data of *Carya spp.* at LE for both CB and LE initialization and observed inventory data of *Pinus spp.* at CB for both CB and LE initialization. The simulated marsh colonization was from external seed supply at the first year, then from both external seed supply and local reproduction afterward.

Daily soil salinity and water table depth at CB and water table depth at LE were used as external driving factors. We used empirically estimated soil salinity at CB, by regression based on open water level and salinity (Ding et al., 2023b). To estimate water table depth at LE from 1990 to 2019, we obtained the water level of LE at the station in Cleveland (https://tidesandcurrents.noaa.gov/inventory.html?id=9063063, last access: 14 November 2025). We fit a linear correlation between the station water level and the observed water table depth at the LE shoreline

location in 2022 (Fig. 1a), then used this linear model to estimate the daily water depth from 1990 to 2019 via the station water data (Fig. 1a). During the simulation period, two floods occurred at LE (1997–1999 and 2016–2019); at CB, salinity slightly rose around 2002 and 2009, followed by a constant increase after 2012 (Fig. 1d and e).

Root loss was driven by soil hypoxia (indexed by the duration of saturated water content) for LE, and both soil hypoxia and salinity for CB. At LE, the root loss was calculated based on water table depth. The parameters that govern root loss were calibrated based on measured sap flow, leaf water potential, and loss of plant hydraulic conductance (S1). At CB, the additive root loss was estimated from soil salinity because soil salinity is highly coupled with hypoxia at CB, and we used the parameter values from Ding et al. (2023b). Root loss was simulated similarly for both species to explicitly examine the extent to which differences in phenology, leaf and stem physiology, and the lack of species-specific information on hypoxia and salinity tolerance may result in different mortality patterns.

3 Results of numerical experiment

3.1 Inundation impacts on tree physiology and mortality

Inundation had similar impacts on the broadleaf and conifer trees at both LE and CB. Root loss increased over time as water levels rose (Fig. 3a, b). However, root loss differed between sites, particularly after 2015, due to the differences in inundation dynamics. At LE, root loss increased each year as water levels rose, but root growth during periods of low water levels allowed partial recovery. In contrast, the chronic increase in inundation and soil salinity at CB after 2015 led to ongoing root loss because there was less seasonal variation in water level (Fig. 1c and d), and hence no opportunity for recovering root biomass. This difference in root loss between sites resulted in sustained reductions in hydraulic conductance ($k/k_{\rm max}$) at CB after 2015, whereas both species at LE exhibited some recovery each year (Fig. 3c, d).

Despite these site level differences, both LE and CB experienced severe declines in $k/k_{\rm max}$ by the end of the simulation period. Non-structural carbohydrates (NSC) showed only slight variation over the simulation period, suggesting that loss of hydraulic conductance was the primary process underlying mortality (Fig. 3e, f). This is consist with observed %NSC at Lake Erie site (Table S3). Mortality of both the broadleaf and conifer trees increased after 2015, with higher mortality at CB than LE (Fig. 3g, h). Increasing root loss was associated with declining $k/k_{\rm max}$ (Fig. 4a, b) and increased whole-tree mortality (Fig. 4c, d), with no difference between species. The declines in $k/k_{\rm max}$ were strongly associated with increased mortality (Fig. 4).

3.2 Ecosystem consequences of forest loss

3.2.1 Broadleaf simulations at Lake Erie and Chesapeake Bay

We examined the ecosystem-scale consequences of mortality on leaf area index (LAI), gross primary production (GPP), transpiration $(E_{\rm T})$, and root water uptake with the broadleaf simulations at both the LE and CB shoreline sites. In these simulations, the loss of leaf area through inundation-driven tree mortality was compensated by marsh invasion, resulting in stable ecosystem-scale LAI over time (Fig. 5a, b). GPP and $E_{\rm T}$ showed somewhat similar patterns as LAI for both sites, again due to marsh invasion as trees died (Fig. 5c-f). GPP was slightly higher in the shoreline than the upland sites due to the higher GPP of marsh plants, and E_T showed slight declines below the upland sites (Fig. 5b and c). While LAI, GPP, and $E_{\rm T}$ all showed relative stability over time, the loss of trees and the marsh invasion led to large changes in the depths of water uptake at both LE and CB. The change in vegetation dominance associated with tree mortality led to an increase in shallow water uptake and a decline in deep water uptake (Fig. 5g-j).

3.2.2 Conifer simulations at Lake Erie and Chesapeake Bay

The conifer simulations at the shoreline sites at both LE and CB exhibited different patterns than the broadleaf species. LAI, GPP, and $E_{\rm T}$ all declined with tree loss, which was not compensated for due to limited marsh invasion (Fig. 6a–f). There was no change in shallow water uptake with changes in vegetation dominance, but there was a large decline in deep water uptake (Fig. 6g–j). As tree LAI declined with mortality, the increase in shallow water uptake observed for broadleaf species was not observed for the conifer species, whereas both species exhibited declines in deep water uptake (Fig. 6).

4 Discussion

4.1 Summary of Major Findings

We conducted numerical experiments at two coastal sites to investigate the mechanisms driving inundation-driven tree mortality and the subsequent ecosystem impacts and how they differ across tree species and with different inundation regimes. The simulations indicated that root loss was the dominant step driving mortality via hydraulic failure for both species and at both sites (Figs. 3 and 4). Replacement of broadleaf trees by marsh resulted in increased LAI and GPP but reduced $E_{\rm T}$ at both sites (Fig. 5a to f). Replacement of conifer trees by marsh result in reduced LAI, GPP, and $E_{\rm T}$ at both sites (Fig. 6a to f). Transition from forests to marsh shifted root water uptake from deep to shallow soil layers (Figs. 4g, h, 6g, h). Our numerical experiments suggest that

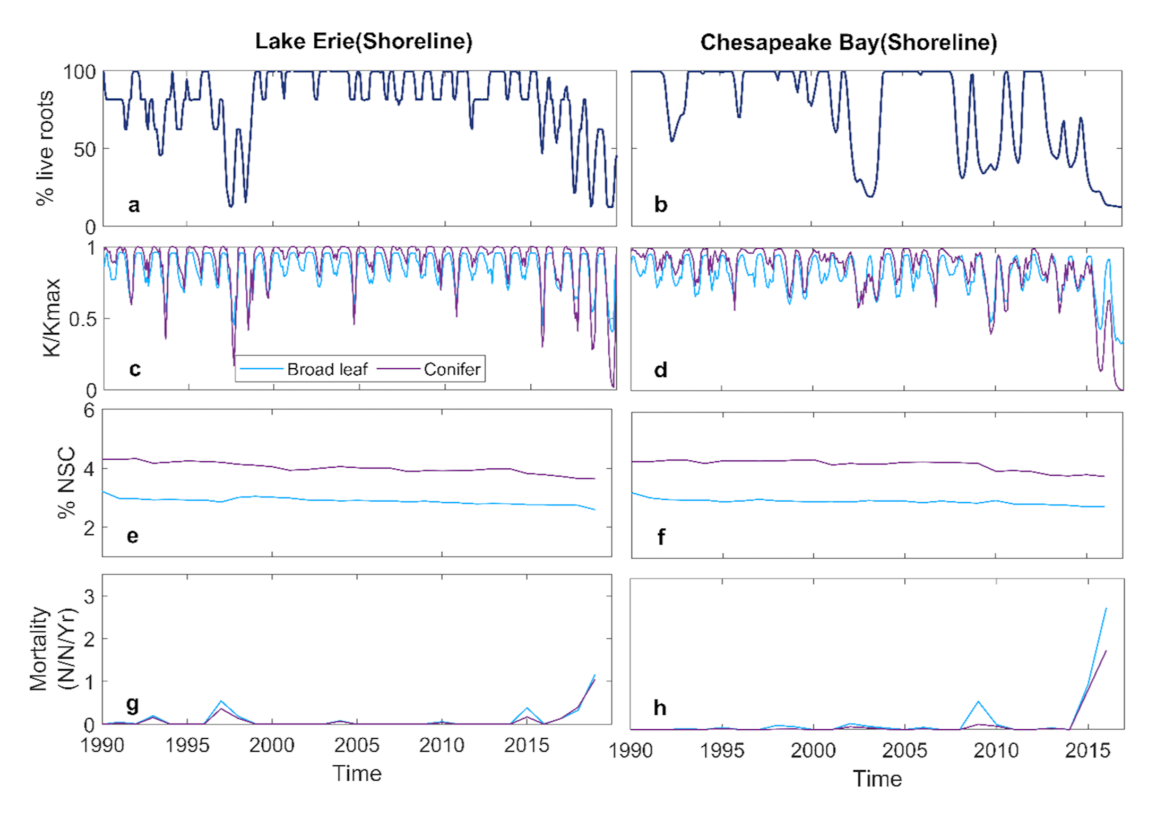


Figure 3. Simulated tree level variables of shoreline forest at Lake Erie and Chesapeake Bay: (\mathbf{a}, \mathbf{b}) monthly mean % live root; (\mathbf{c}, \mathbf{d}) monthly mean k/k_{max} ; (\mathbf{e}, \mathbf{f}) annual %NSC; (\mathbf{g}, \mathbf{h}) annual mortality rate.

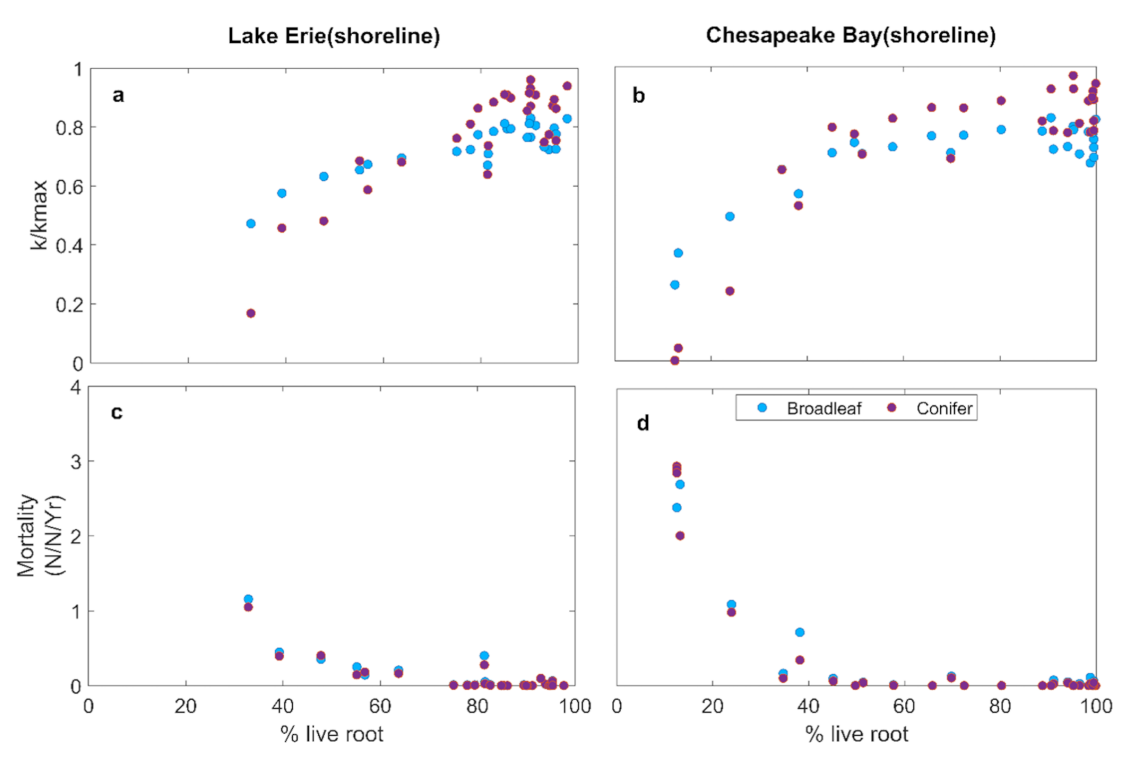


Figure 4. Simulated relation between (\mathbf{a}, \mathbf{b}) mean growing season k/k_{max} and % live roots of tree; (\mathbf{c}, \mathbf{d}) annual mean mortality and % live roots of tree.

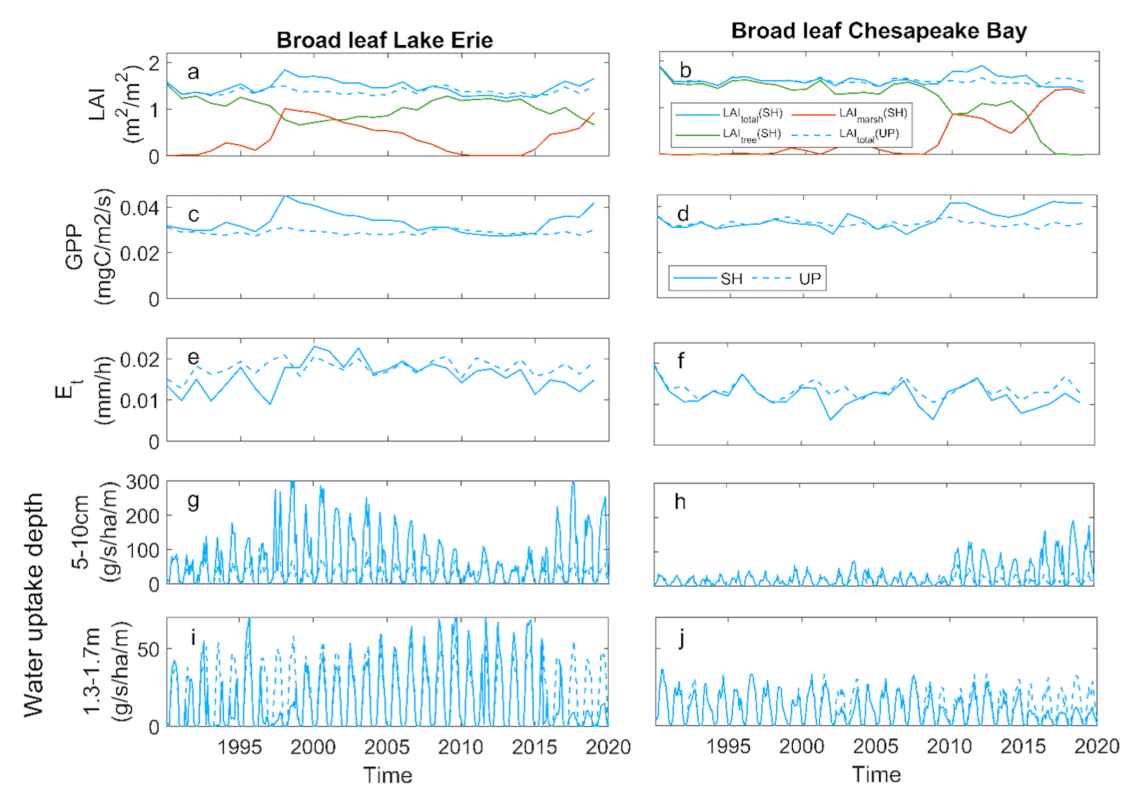


Figure 5. Ecosystem effects of broadleaf forest at Lake Erie and Chesapeake Bay: (\mathbf{a}, \mathbf{b}) mean growing season leaf area index (LAI); (\mathbf{c}, \mathbf{d}) gross primary productivity (GPP); (\mathbf{e}, \mathbf{f}) transpiration (E_T) ; (\mathbf{g}, \mathbf{h}) root water uptake rate from shallow soil; (\mathbf{i}, \mathbf{j}) root water uptake rate from deep soil at shoreline (SH) and upland (UP) locations.

the same mechanisms caused forest loss at both sites regardless of tree type, whereas the ecosystem effects from the replacement of forest by marsh differed between broadleaf and conifer forests. Future empirical studies should be conducted to verify these findings.

4.2 Tree Level Effects

Root loss can promote tree mortality through hydraulic failure and carbon starvation (McDowell et al., 2022). Our simulations indicated that hydraulic failure is the dominant process underlying tree mortality for broadleaf and conifer trees at both sites (Figs. 3 and 4). Root loss resulted in decreased whole tree hydraulic conductance and subsequently xylem conductivity due to increased xylem embolism (Fig. 4a and b). Overall, this led to an increase in tree mortality (Fig. 4c and d). These effects were consistent between LE and CB, although they exhibited different temporal patterns due to variation in the inundation regimes. Moreover, similar effects of root loss on plant hydraulics have been documented in both modeling studies (Li et al., 2021; Ding et al., 2023b) and field studies (Zaerr, 1983; Pezeshki et al., 1996; Andersen et al., 1984; Islam and Macdonald, 2004; Aroca et al., 2012; Karlova et al., 2021).

Reduced hydraulic conductivity can lower leaf water potential and causes stomatal closure. This mechanism can result in reduced photosynthesis and negative carbon balance, resulting in reduced capability to maintain tissues and defend against insects and pathogens (McDowell et al., 2022). However, simulated non-structural carbohydrates (NSC) values (Fig. 3e and f) suggest that carbon starvation was not a major process of tree mortality at the shoreline locations of both study sites and for both tree types. We had anticipated that broadleaf trees might experience greater carbon limitation due to higher leaf area and photosynthetic demand. However, the simulations demonstrated that hydraulic failure associated with root loss occurred before significant depletion of NSC, leading to similar mortality trajectories between the two species. This may be due to the rate of inundationdriven root loss relative to the rate of NSC decline (Ding et al., 2023b). The LE and CB inundation regimes had periods when inundation declined and the salinity at CB was relatively low, allowing a low level of ongoing photosynthesis to replenish their NSC pools. Carbon starvation is a slow process due to the time required to draw down NSCs, whereas hydraulic failure can occur rapidly (McDowell et al., 2022).

Simulated k/k_{max} and mortality of broadleaf and conifer trees changed similarly with root loss (Fig. 4), despite large differences in their leaf economic traits, wood anatomy,

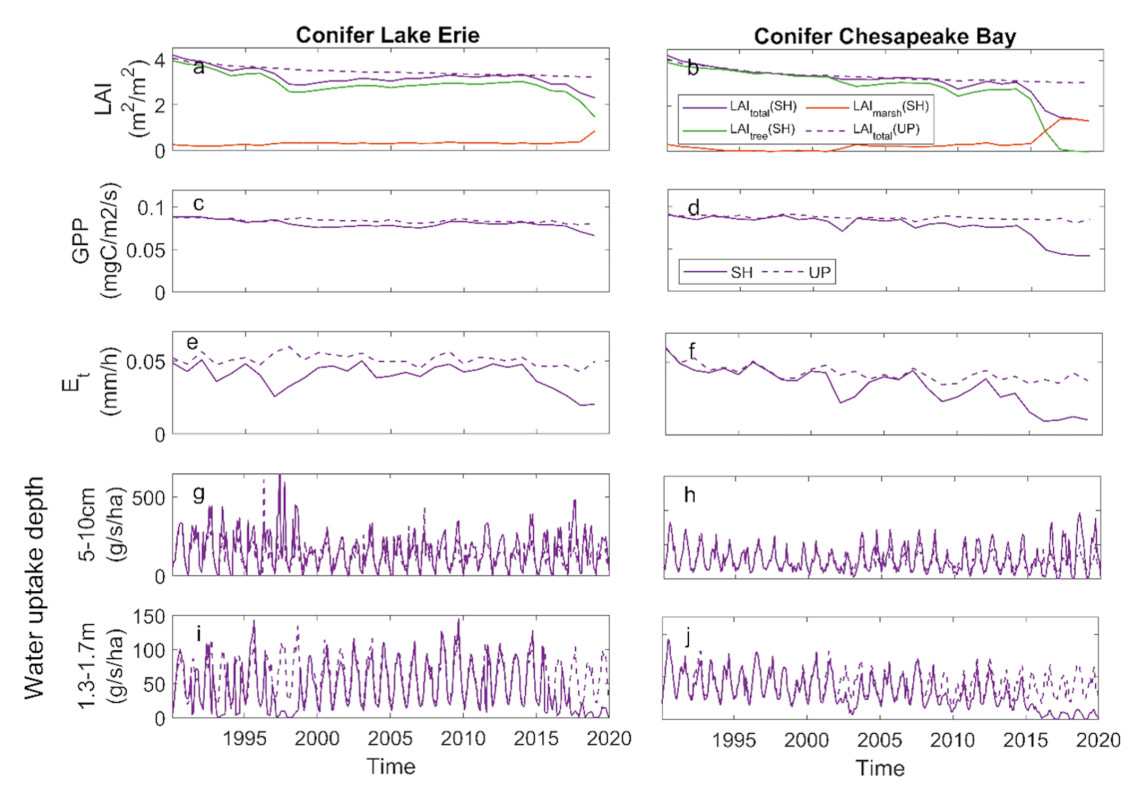


Figure 6. Ecosystem effects of conifer forest at Lake Erie and Chesapeake Bay: (\mathbf{a} , \mathbf{b}) mean growing season leaf area index (LAI); (\mathbf{c} , \mathbf{d}) gross primary productivity (GPP); (\mathbf{e} , \mathbf{f}) transpiration (E_T); (\mathbf{g} , \mathbf{h}) root water uptake rate from shallow soil;(\mathbf{i} , \mathbf{j}) root water uptake rate from deep soil at shoreline (SH) and upland (UP) locations.

crown allometry, and phenology. This similarity arose because whole-tree k/k_{max} can only be as high as the lowest $k/k_{\rm max}$ of any pathway between the soil and foliage. Wholetree hydraulic conductance is constrained by the lowest conductance along the soil-plant-atmosphere pathway. In our simulations, root loss strongly reduced soil-to-root conductance, which therefore set the limit for whole-tree k/k_{max} . Thus, traits and processes downstream from the roots became less important due to the dominant role of root loss in promoting hydraulic failure when it becomes severe (Fig. 3c, d, g, h). Both species are poorly adapted to high levels of hypoxia or salinity, thus root loss was the critical failure point in tree survival under inundation. Species with root systems adapted to inundation, such as mangroves, may experience different consequences of increased flooding that could lead to a larger role of carbon starvation such as through ion toxicity to photosynthesis and leaf loss (Munns and Termaat, 1986).

This convergence in response does not imply that all species react identically to inundation. Rather, it reflects that under the modeled conditions, root system failure overwhelms the contributions of other physiological differences. While these results offer mechanistic insights, the lack of empirical data on species-specific root adaptations remains a limitation. We note that our parameterizations were based

on representative species (Carya, Quercus, and Pinus), which we treated as proxies for the two tree types. Outcomes may differ among other species within these groups, therefore we caution against overgeneralization and recommend interpreting these results as hypothesis-generating rather than conclusive. Future research on the cross-species variation of root loss and downstream mortality mechanisms, and explicitly test whether these findings extend to the broader PFT level, will be useful to advance transferable predictive capacity of coastal vegetation change under increasing inundation.

4.3 Ecosystem-Level Effects Between the Forest Types and Sites

The ecosystem-scale consequences of coastal forest loss result both from the loss of trees and the invasion of marsh plants. We found differences in the ecosystem consequences associated with species but not sites. As tree mortality associated with soil inundation and/or salinity progressed, marsh plants invaded broadleaf systems more rapidly than coniferous systems, thus resulting in different impacts on GPP and $E_{\rm T}$. Marsh plants invaded when LAI declined below 1 m² m⁻² in both systems (Figs. 5a, b and 6a, b). The conifer system had higher stand density than the broadleaf system resulting in initial LAI values of \sim 4 and \sim 2 m² m⁻², respectively, thus a much larger amount of mortality was re-

quired in the conifer system for LAI to decline by 1 m² m⁻²; in other words, when canopy opened hereby facilitated marsh invasion and establishment. The mortality rates were similar for both species (Fig. 3); thus, the differences in marsh invasion were due primarily to initial stand structure rather than to species composition or mortality rates per se. The declining LAI in the CB with increasing mortality is consistent with remotely sensed estimates of the normalized difference vegetation index (Chen and Kirwan, 2022b), and the rates of marsh invasion are consistent with other observations (Kirwan and Gedan, 2019; McKown and Burdick, 2024). This resulted in increasing GPP in the broadleaf system because marsh plants have higher photosynthetic capacity than trees (Pan et al., 2020) and because ecosystem LAI was higher after marsh invasion into the broadleaf system (Figs. 5c, d and 6c, d). In contrast, the slower invasion of marsh plants into the conifer system caused ecosystem level GPP to decline with tree mortality.

Replacing broadleaf forest by marsh increased GPP slightly, while $E_{\rm T}$ declined slightly (Fig. 7c and d). This is likely due to the higher water-use efficiency of marsh plants than trees. $E_{\rm T}$ declined with tree mortality in both systems, but more so in the conifer system (Figs. 5e, f and 6e, f). These changes were associated with increased water uptake from shallow soil layer and reduced uptake from the deep soil layer due to the shallower roots of the marsh plants (Fig. 8) (Le Maitre et al., 1999; Schenk and Jackson, 2002). In contrast, conifer mortality resulted in less marsh invasion and hence reductions in GPP and $E_{\rm T}$ (Fig. 7), and water uptake from both shallow and deep soil layers was greatly reduced due to the loss in conifer roots that were not compensated by marsh plants (Fig. 8).

4.4 Future Research

Our numeric experiments revealed critical mechanisms regulating vegetation dynamics and ecosystem impacts in response to SLR. Our study also revealed key next steps to improve our understanding and model representation. We found that root loss drives large declines in k/k_{max} that result in increasing mortality and marsh invasion. However, we did not directly measure root distribution, but instead calibrated parameters using observed data on leaf water potential, sap flow, and the $k/k_{\rm max}$. We then applied these calibrated parameters with the assumption that both the broadleaf and conifer had similar root responses to hypoxia and salinity. This decision was based on three factors. First, we had no species-specific data on root conductance and mortality in response to hypoxia and salinity. Second, both species live at the shoreline margins of their respective regions, and thus, we assume they are similar in their root responses. Third, the rooting depths at both sites are shallow, thus rooting depth may not vary significantly across species. By setting the root loss parameters the same for both tree species, we investigated whether differences in phenology, leaf and stem physiology traits result in different mortality patterns between the two species and found that these trait differences have negligible impacts. Given the critical role of root conductance and survival, field studies to explore root structure and function are important next steps for coastal systems. Ecosystem manipulation experiments can be particularly powerful to untangle the impact of hypoxia and salinity on root loss and subsequent impacts on physiology and survival, enabling causeand-effect tests that enable improved predictive understanding of tree mortality in coastal systems (e.g., Hopple et al., 2023).

The role of changing stand structure during ghost forest formation may be an important factor impacting marsh invasion, the physiology of surviving trees, and the recruitment of new trees. Changes in light availability as mortality increases aided marsh invasion and promoted higher photosynthesis and recruitment (Figs. 5a and b, 6a and b) (Kirwan and Gedan, 2019). The reduction of water uptake from deep layers may promote hypoxia, salinity, and changes in redox potential and nutrient cycling. With forest cover, high deepwater uptake can enhance infiltration of rainfall into deep soil layers, which can bring oxygen rich surface water and nutrients to these deep layers. Reduced infiltration could result in lower dissolved oxygen in deep soil (Foulquier et al., 2010), increased salinity (Kirwan et al., in review), changed redox potential (Rubol et al., 2012), and decreased nutrient availability (Burgin and Groffman, 2012) all of which should feedback to limit vegetation growth. Therefore, quantifying the rate of marsh invasion, survival of remaining trees, and recruitment of tree seedlings is necessary to identify mechanisms associated with changing light availability and belowground processes.

In addition, it is important to interpret our results in the context of projected future climate change and sea-level rise. Chesapeake Bay is expected to continue experiencing sea-level rise of approximately 3-6 mm yr⁻¹, about twice the global average, while the Great Lakes are projected to undergo increasingly variable water levels under climate change (Kayastha et al., 2022; Sallenger et al., 2012; Ezer and Corlett, 2012). These projections imply that inundation events will become more frequent and prolonged, thereby intensifying the mechanisms identified in our study, particularly root loss leading to hydraulic failure. Rising temperatures and elevated CO2 may further modify these dynamics by altering tree water demand, photosynthetic rates, and marsh productivity, though the net effects remain uncertain. Together, these changes suggest heightened vulnerability of both broadleaf and conifer coastal forests to conversion into marshes, with ecosystem-scale consequences for carbon cycling and hydrology. These broader climate-hydrology interactions are examined in more detail in a separate manuscript (Ding et al., 2025), where we provide more detailed projections.

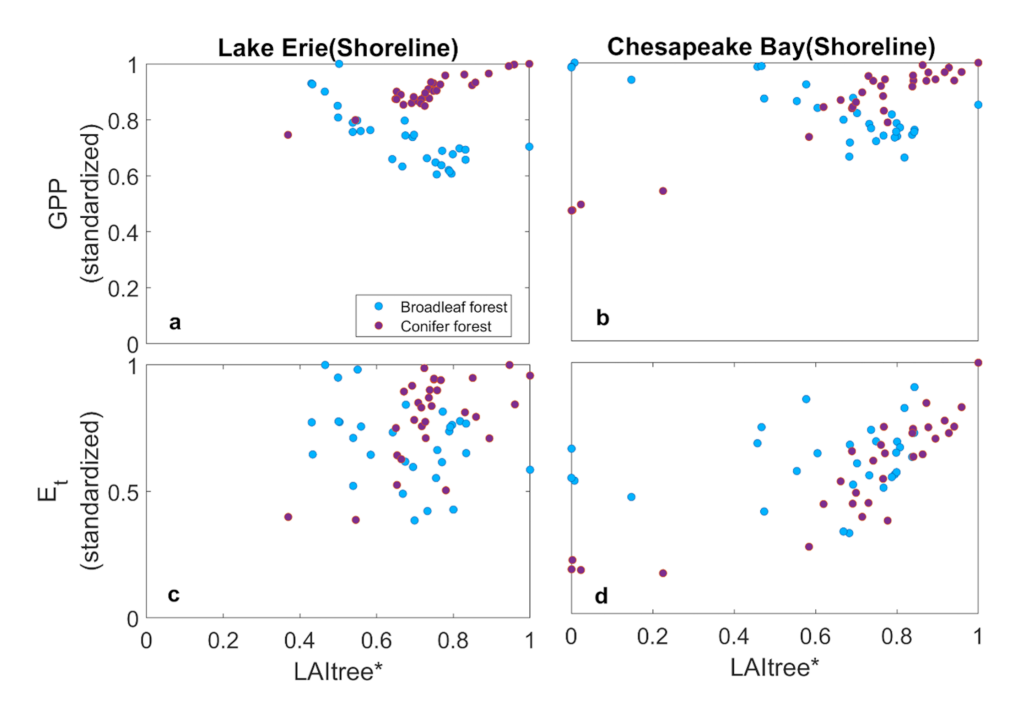


Figure 7. Change in gross primary productivity (GPP) (\mathbf{a} , \mathbf{b}) and transpiration (E_T) (\mathbf{c} , \mathbf{d}) with tree abundance of shoreline forests as indicated by tree LAI at Lake Erie and Chesapeake Bay.

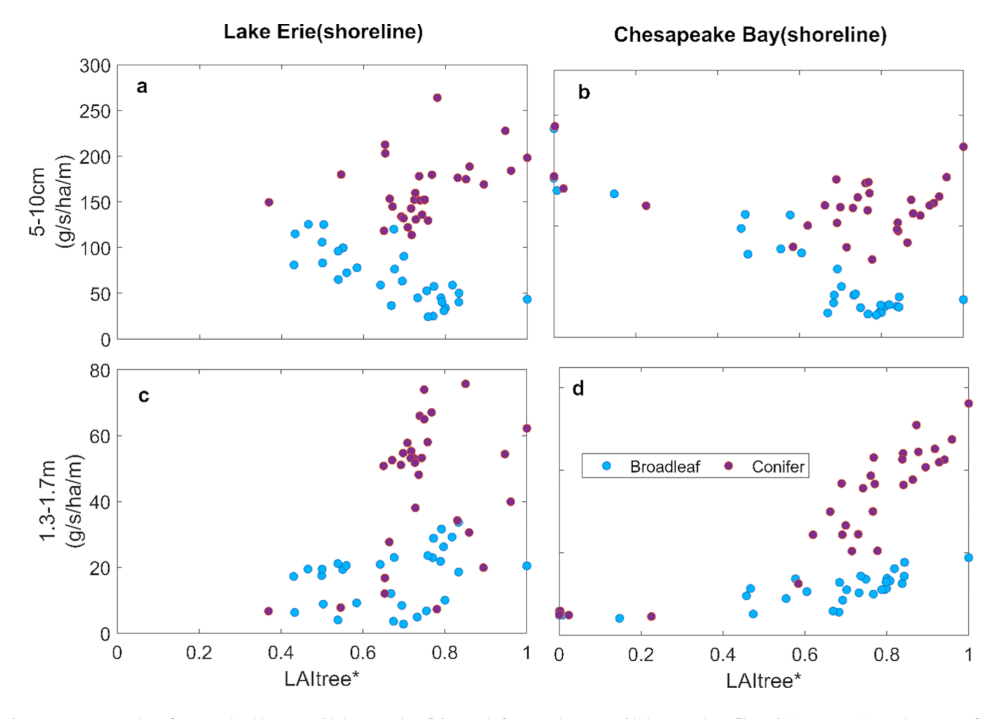


Figure 8. Change in water uptake from shallow soil layer (a, b) and from deep soil layer (c, d) with tree abundance of shoreline forests as indicated by tree LAI at Lake Erie and Chesapeake Bay.

4.5 Summary

Our numerical experiments indicated that root loss due to coastal inundation served as the driving force behind the transition from forest to marsh through hydraulic failure-induced tree mortality. This mechanism resulted in similar physiological consequences for both broadleaf and conifer trees. However, the transition from forests to marshes led to different ecosystem impacts between broadleaf and conifer forests due to their different initial LAI. Future research aimed at

enhancing our understanding and representation of the interplay among physiological, demographic, and stand structural processes in different forest types is necessary for better predicting vegetation dynamics and ecosystem consequences under SLR.

Code and data availability. The data and FATES-Hydro code that support the findings of this study are openly available in GitHub repository: https://github.com/JunyanDing/FATES_COMPASS (last access: 14 November 2025) or Zenodo: https://doi.org/10.5281/zenodo.15116449 (Ding, 2025).

Supplement. The supplement related to this article is available online at https://doi.org/10.5194/bg-22-6963-2025-supplement.

Competing interests. The contact author has declared that none of the authors has any competing interests.

Disclaimer. Publisher's note: Copernicus Publications remains neutral with regard to jurisdictional claims made in the text, published maps, institutional affiliations, or any other geographical representation in this paper. While Copernicus Publications makes every effort to include appropriate place names, the final responsibility lies with the authors. Views expressed in the text are those of the authors and do not necessarily reflect the views of the publisher.

Author contributions. JD and NM designed the study and drafted the manuscript. JD developed the model and performed simulations. CDK helped with model development. NM, NW, LS, DD, KM, MK, PR, PZ, HZ, SP, SW, WW, WI, AS, TM, and PT collected field data and performed data analysis. All the authors contributed to the manuscript.

Acknowledgements. JD, NM, BBL, KM, NW, JPM, PR, SCP, MW, TM, PT, and VB were supported by the Department of Energy, Biological and Environmental Research program project Coastal Observations, Mechanisms, and Predictions Across Scales (COMPASS). Any use of trade, product or firm names is for descriptive purposes only and does not imply endorsement by the U.S. Government. MK acknowledges the support of the U.S. National Science Foundation (grant nos. 1654374, 1832221, 2012670).

Financial support. This research has been supported by the U.S. Department of Energy (grant no. 2012671) and the National Science Foundation (grant nos. 1654374, 1832221, and 2012670).

Review statement. This paper was edited by Marijn Bauters and reviewed by Steven De Hertog and Ronny Peters.

References

- Acosta-Motos, J. R., Ortuño, M. F., Bernal-Vicente, A., Diaz-Vivancos, P., Sanchez-Blanco, M. J., and Hernandez, J. A.: Plant responses to salt stress: Adaptive mechanisms, Agronomy, 7, 18, https://doi.org/10.3390/agronomy7010018, 2017.
- Andersen, P. C., Lombard, P. B., Westwood, M. N.: Effects of root anaerobiosis on the water relations of several Pyrus species, Physiol. Plant, 62, 245–252, 1984.
- Arkema, K. K., Guannel, G., Verutes, G., Wood, S. A., Guerry, A., Ruckelshaus, M., Kareiva, P., Lacayo, M., and Silver, J. M.: Coastal habitats shield people and property from sea-level rise and storms, Nat. Clim. Change, 3, 913–918, 2013.
- Aroca, R., Porcel, R., and Ruiz-Lozano, J. M.: Regulation of root water uptake under abiotic stress conditions, J. Exp. Bot., 63, 43–57, https://doi.org/10.1093/jxb/err266, 2012.
- Ball, M. C., and Farquhar, G. D.: Photosynthetic and stomatal responses of two mangrove species, Aegiceras corniculatum and Avicennia marina, to long term salinity and humidity conditions, Plant Physiology, 74, 1–6, 1984.
- Ball, M. C., Farquhar, G. D., and Box, P. O.: Photosynthetic and stomatal responses of two mangrove species, Aegiceras corniculatum and Avicennia marina, to long-term salinity and humidity conditions, Plant Physiol., 74,1 https://academic.oup.com/plphys/article/74/1/1/6079345, 1984.
- Barbier, E. B.: Valuing ecosystem services for coastal wetland protection and restoration: Progress and challenges, Resources, 2, 213–230, 2013.
- Barbier, E. B., Hacker, S. D., Kennedy, C., Koch, E. W., Stier, A. C., and Silliman, B. R.: The value of estuarine and coastal ecosystem services, Ecol. Monogr., 81, 169–193, 2011.
- Boursiac, Y., Chen, S., Luu, D.-T., Sorieul, M., van den Dries, N., and Maurel, C.: Early effects of salinity on water transport in Arabidopsis roots. Molecular and cellular features of aquaporin expression, Plant Physiology, 139, 790–805, https://doi.org/10.1104/pp.105.065029, 2005.
- Brennan, M. J., Criscione, K. S., Olichney, J. A., Ding, J., Fang, Y., McDowell, N., and Wolfe, B. T.: Hydraulic constraints to stomatal conductance in flooded trees, Oecologia, 207, 1–4, https://doi.org/10.1007/s00442-025-05789-y, 2025.
- Burgin, A. J., and Groffman P. M.: Soil O₂ controls denitrification rates and N₂O yield in a riparian wetland, Journal of Geophysical Research, Biogeosciences, 117, https://doi.org/10.1029/2011JG001799, 2012.
- Burlakova, L. E., Karatayev, A. Y., Pennuto, C., and Mayer, C.: Changes in Lake Erie benthos over the last 50 years: Historical perspectives, current status, and main drivers, J. Great Lakes Res., 40, 560–573, 2014.
- Chen, Y., and Kirwan, M. L.: Climate-driven decoupling of wetland and upland biomass trends on the mid-Atlantic coast, Nat. Geosci., 15, 913–918, https://doi.org/10.1038/s41561-022-01041-x, 2022a.
- Chen, Y., and Kirwan, M. L.: A phenology- and trend-based approach for accurate mapping of sea-level driven coastal forest retreat, Remote Sensing of Environment, 281, https://doi.org/10.1016/j.rse.2022.113229, 2022b.
- Christoffersen, B. O., Gloor, M., Fauset, S., Fyllas, N. M., Galbraith, D. R., Baker, T. R., Kruijt, B., Rowland, L., Fisher, R. A., Binks, O. J., Sevanto, S., Xu, C., Jansen, S., Choat, B., Mencuccini, M., McDowell, N. G., and Meir, P.: Linking hydraulic

- traits to tropical forest function in a size-structured and trait-driven model (TFS v.1-Hydro), Geosci. Model Dev., 9, 4227–4255, https://doi.org/10.5194/gmd-9-4227-2016, 2016.
- Clough, B. F., and Sim, R. G.: Changes in gas exchange characteristics and water use efficiency of mangroves in response to salinity and vapour pressure deficit, Oecologia, 79, 38–44, 1989.
- Colmer, T. D., and Flowers, T. J.: Flooding tolerance in halophytes, New Phytologist, 179, 964–974, 2008.
- Davidson, I. C., Cott, G. M., Devaney, J. L., and Simkanin, C.: Differential effects of biological invasions on coastal blue carbon: A global review and meta-analysis, Glob. Change Biol., 24, 5218–5230, 2018.
- Delatorre-Herrera, J., Ruiz, K. B., and Pinto, M.: The importance of non-diffusional factors in determining photosynthesis of two contrasting quinoa ecotypes (Chenopodium quinoa Willd.) subjected to salinity conditions, Plants, 10, 927, 2021.
- Ding, J.: FATES-Hydro codes, Zenodo [code], https://doi.org/10.5281/zenodo.15116449, 2025.
- Ding, J., Buotte, P., Bales, R., Christoffersen, B., Fisher, R. A., Goulden, M., Knox, R., Kueppers, L., Shuman, J., Xu, C., and Koven, C. D.: Coordination of rooting, xylem, and stomatal strategies explains the response of conifer forest stands to multi-year drought in the southern Sierra Nevada of California, Biogeosciences, 20, 4491–4510, https://doi.org/10.5194/bg-20-4491-2023, 2023a.
- Ding, J., McDowell, N., Fang, Y., Ward, N., Kirwan, M. L., Regier, P., Megonigal, P., Zhang, P., Zhang, H., Wang, W., and Li, W.: Modeling the mechanisms of conifer mortality under seawater exposure, New Phytol., https://doi.org/10.1111/nph.19076, 2023b.
- Ding, J., McDowell, N., Conroy, N., Day, D. J., Fang, Y., Kemner, K. M., Kirwan, M. L., Kovach, M., Megonigal, P., Morris, K. A., O'Meara, T., Pennington, S. C., Peixoto, R. B., Thornton, P., Weintraub, M., Regier, P., Sandoval, L., Machado-Silva, F., Stearns, A., Ward, N. D., Wilson, S. J., and Bailey, V.: Investigating coastal vegetation dynamics and ecosystem impacts under elevated CO₂ and temperature: a mechanistic modeling approach, J. Geophys. Res.-Biogeo., in review, 2025.
- Duarte, C. M., Losada, I. J., Hendriks, I. E., Mazarrasa, I., and Marbà, N.: The role of coastal plant communities for climate change mitigation and adaptation, Nat. Clim. Change, 3, 961– 968, 2013.
- Ezer, T. and Corlett, W. B.: Analysis of relative sea-level variations and trends in the Chesapeake Bay: Is there evidence for acceleration in sea level rise?, in: Proc. MTS/IEEE Oceans 2012, Hampton Roads, USA, 14–19 October 2012, https://doi.org/10.1109/OCEANS.2012.6404930, 2012.
- Falster, D. S., Duursma, R. A., Ishihara, M. I., Barneche, D. R., Fitzjohn, R. G., Rhammar, A. V., Aiba, M., Ando, M., Anten, N., Aspinwall, M. J., Baltzer, J. L., Baraloto, C., Battaglia, M., Battles, J. J., Bond-Lamberty, B., van Breugel, M., Camac, J., Claveau, Y., Coll, L., Dannoura, M., Delagrange, S., Domec, J.-C., Fatemi, F., Feng, W., Gargaglione, V., Goto, Y., Hagihara, A., Hall, J. S., Hamilton, S., Harja, D., Hiura, T., Holdaway, R., Hutley, L. S., Ichie, T., Jokela, E. J., Kantola, A., Kelly, J. W. G., Kenzo, T., King, D., Kloeppel, B. D., Kohyama, T., Komiyama, A., Laclau, J.-P., Lusk, C. H., Maguire, D. A., le Maire, G., Mäkelä, A., Markesteijn, L., Marshall, J., McCulloh, K., Miyata, I., Mokany, K., Mori, S., Myster, R. W., Nagano, M., Naidu,

- S. L., Nouvellon, Y., O'Grady, A. P., O'Hara, K. L., Ohtsuka, T., Osada, N., Osunkoya, O. O., Peri, P. L., Petritan, A. M., Poorter, L., Portsmuth, A., Potvin, C., Ransijn, J., Reid, D., Ribeiro, S. C., Roberts, S. D., Rodríguez, R., Saldaña-Acosta, A., Santa-Regina, I., Sasa, K., Galia Selaya, N., Sillett, S. C., Sterck, F., Takagi, K., Tange, T., Tanouchi, H., Tissue, D., Umehara, T., Utsugi, H., Vadeboncoeur, M. A., Valladares, F., Vanninen, P., Wang, J. R., Wenk, E., Williams, R., de Aquino Ximenes, F., Yamaba, A., Yamada, T., Yamakura, T., Yanai, R. D., and York, R. A.: BAAD: a Biomass And Allometry Database for woody plants, Ecological Archives, 96–128, in: Data Papers Ecology, 96, https://doi.org/10.6084/m9.figshare.c.3307692.v1 (last access: 17 November 2025), 2015.
- FATES Development Team: The Functionally Assembled Terrestrial Ecosystem Simulator (FATES) (fates-clm-v0.2-Junyan), Zenodo [data set], https://doi.org/10.5281/zenodo.5504405, 2023.
- Fisher, R. A., Muszala, S., Verteinstein, M., Lawrence, P., Xu, C., McDowell, N. G., Knox, R. G., Koven, C., Holm, J., Rogers, B. M., Spessa, A., Lawrence, D., and Bonan, G.: Taking off the training wheels: the properties of a dynamic vegetation model without climate envelopes, CLM4.5(ED), Geosci. Model Dev., 8, 3593–3619, https://doi.org/10.5194/gmd-8-3593-2015, 2015.
- Fisher, R. A., Koven, C. D., Anderegg, W. R. L., Christoffersen, B. O., Dietze, M. C., Farrior, C. E., Holm, J. A., Hurtt, G. C., Knox, R. G., Lawrence, P. J., Lichstein, J. W., Longo, M., Matheny, A. M., Medvigy, D., Muller-Landau, H. C., Powell, T. L., Serbin, S. P., Sato, H., Shuman, J. K., Smith, B., Trugman, A. T., Viskari, T., Verbeeck, H., Weng, E., Xu, C., Xu, X., Zhang, T., and Moorcroft, P. R.: Vegetation demographics in Earth System Models: A review of progress and priorities, Glob. Change Biol., 24, 35–54, https://doi.org/10.1111/gcb.13910, 2018.
- Foulquier, A., Malard, F., Mermillod-Blondin, F., Datry, T., Simon, L., Montuelle, B., and Gibert, J.: Vertical change in dissolved organic carbon and oxygen at the water table region of an aquifer recharged with stormwater: biological uptake or mixing?, Biogeochemistry, 99, 31–47, 2010.
- Frieswyk, C. B. and Zedler, J. B.: Vegetation change in Great Lakes coastal wetlands: Deviation from the historical cycle, J. Great Lakes Res., 33, 366–380, 2007.
- Harris, I. C.: CRU JRA v2.1: A forcings dataset of gridded land surface blend of Climatic Research Unit (CRU) and Japanese reanalysis (JRA) data; Jan.1901 Dec.2019, Centre for Environmental Data Analysis [data set], https://doi.org/10.5285/13f3635174794bb98cf8ac4b0ee8f4ed, 2019.
- Hopple, A. M., Doro, K. O., Bailey, V. L., Bond-Lamberty, B., Mc-Dowell, N., Morris, K. A., Myers-Pigg, A., Pennington, S. C., Regier, P., Rich, R., Sengupta, A., Smith, R., Stegen, J., Ward, N. D., Woodard, S. C., and Megonigal, J. P.: Attaining freshwater and estuarine-water soil saturation in an ecosystem-scale coastal flooding experiment, Environ. Monit. Assess., 195, 425, https://doi.org/10.1007/s10661-022-10807-0, 2023.
- Hudon, C.: Impact of water level fluctuations on St. Lawrence River aquatic vegetation, Can. J. Fish. Aquat. Sci., 54, 2853–2865, 1997.
- Islam, M. A. and Macdonald, S. E.: Ecophysiological adaptations of black spruce (Picea mariana) and tamarack (Larix laricina) seedlings to flooding, Trees, 18, 35–42, 2004.

- Karlova, R., Boer, D., Hayes, S., and Testerink, C.: Root plasticity under abiotic stress, Plant Physiol., 187, 1057–1070, 2021.
- Kattge, J., Bönisch, G., Díaz, S., Lavorel, S., Prentice, I. C., Leadley, P., Tautenhahn, S., Werner, G., et al.: TRY Plant Trait Database–Enhanced Coverage and Open Access, Glob. Change Biol., 26, 119–188, 2020.
- Kayastha, M. B., Ye, X., Huang, C., and Xue, P.: Future rise of the Great Lakes water levels under climate change, J. Hydrol., 612, 128205, https://doi.org/10.5539/jsd.v18n2p15, 2022.
- Keddy, P. A. and Reznicek, A. A.: Great Lakes vegetation dynamics: The role of fluctuating water levels and buried seeds, J. Great Lakes Res., 12, 25–36, 1986.
- Kirwan, M. L., and Gedan, K. B.: Sea-level driven land conversion and the formation of ghost forests, Nature Climate Change, 9, 450–457, 2019.
- Kirwan, M. L., Megonigal, J. P., Noyce, G. L., and Smith, A. J.: Geomorphic and ecological constraints on the coastal carbon sink, Nature Reviews Earth & Environment, 4, 393–406, https://doi.org/10.1038/s43017-023-00429-6, 2023.
- Koven, C. D., Knox, R. G., Fisher, R. A., Chambers, J. Q., Christoffersen, B. O., Davies, S. J., Detto, M., Dietze, M. C., Faybishenko, B., Holm, J., Huang, M., Kovenock, M., Kueppers, L. M., Lemieux, G., Massoud, E., McDowell, N. G., Muller-Landau, H. C., Needham, J. F., Norby, R. J., Powell, T., Rogers, A., Serbin, S. P., Shuman, J. K., Swann, A. L. S., Varadharajan, C., Walker, A. P., Wright, S. J., and Xu, C.: Benchmarking and parameter sensitivity of physiological and vegetation dynamics using the Functionally Assembled Terrestrial Ecosystem Simulator (FATES) at Barro Colorado Island, Panama, Biogeosciences, 17, 3017–3044, https://doi.org/10.5194/bg-17-3017-2020, 2020.
- Kirwan, M. L. and Gedan, K. B.: Sea-level driven land conversion and the formation of ghost forests, Nat. Clim. Change, 9, 450– 457, 2019.
- Le Maitre, D. C., Scott, D. F., and Colvin, C.: Review of information on interactions between vegetation and groundwater, Water SA, 25, 137–152, https://researchspace.csir.co.za/server/api/core/bitstreams/ff784773-53a0-49d9-ab1f-34f936da5954/content (last access: 19 November 2025), 1999.
- Li, W., Zhang, H., Wang, W., Zhang, P., Ward, N. D., Norwood, M., Myers-Pigg, A., Zhao, C., Leff, R., Yabusaki, S., Waichler, S., Bailey, V. L., and McDowell, N. D.: Changes in carbon and nitrogen metabolism during seawater-induced mortality of *Picea sitchensis* trees, Tree Physiology, 41, 2326–2340, https://doi.org/10.1093/treephys/tpab073, 2021.
- López-Berenguer, C., Garcia-Viguera, C., and Carvajal, M.: Are root hydraulic conductivity responses to salinity controlled by aquaporins in broccoli plants?, Plant and Soil, 279, 13–23, 2006.
- Manzoni, S.: Integrating plant hydraulics and gas exchange along the drought-response trait spectrum, Tree Physiol., 34, 1031– 1034, https://doi.org/10.1093/treephys/tpu088, 2014.
- McDowell, N. G., Ball, M., Bond-Lamberty, B., Kirwan, M. L., Krauss, K. W., Megonigal, J. P., Mencuccini, M., Ward, N. D., Weintraub, M. N., and Bailey, V.: Processes and mechanisms of coastal woody-plant mortality, Glob. Change Biol., 28, 5881–5900, https://doi.org/10.1111/gcb.16297, 2022.
- McKown, J. G. and Burdick, D. M.: Salt marsh migration into coastal uplands and application for conservation in New Hampshire, Great Bay National Estuarine Research Reserve, 45

- pp., https://scholars.unh.edu/jel/681/ (last access: 14 November 2025), 2024.
- Mimura, N.: Sea-level rise caused by climate change and its implications for society, Proc. Jpn. Acad. Ser. B, 89, 281–301, 2013.
- Mitsch, W. J., Bernal, B., and Hernandez, M. E.: Ecosystem services of wetlands, Int. J. Biodivers. Sci. Ecosyst. Serv. Manag., 11, 1–4, 2015.
- Munns, R.: Genes and salt tolerance: bringing them together, New phytologist, 167, 645–663, 2005.
- Munns, R. and Termaat, A.: Whole-plant responses to salinity, Funct. Plant Biol., 13, 143–160, 1986.
- Nedjimi, B.: Effects of salinity on growth, membrane permeability and root hydraulic conductivity in three saltbush species, Biochemical Systematics and Ecology, 52, 4–13, 2014.
- Niknam, S. R. and McComb, J.: Salt tolerance screening of selected Australian woody species a review, For. Ecol. Manage., 139, 1–19, 2000.
- Oleson, K. W., Lawrence, D. M., Bonan, G. B., Drewniak, B., Huang, M., Koven, C. D., and Yang, Z.: Technical description of version 4.5 of the Community Land Model (CLM), NCAR Technical Note, https://opensky.ucar.edu/islandora/object/technotes: 515 (last access: 14 November 2025), 2013.
- O'Meara, T. A., Thornton, P. E., Ricciuto, D. M., Noyce, G. L., Rich, R. L., and Megonigal, J. P.: Considering coasts: Adapting terrestrial models to characterize coastal wetland ecosystems, Ecol. Model., 450, 109561, https://doi.org/10.1016/j.ecolmodel.2021.109561, 2021.
- Orsini, F., Alnayef, M., Bona, S., Maggio, A., and Gianquinto, G.: Low stomatal density and reduced transpiration facilitate strawberry adaptation to salinity, Environmental and Experimental Botany, 81, 1–10, https://doi.org/10.1016/j.envexpbot.2012.02.005, 2012.
- Pan, Y., Cieraad, E., Armstrong, J., Armstrong, W., Clarkson, B. R., Colmer, T. D., Pedersen, O., Visser, E. J. W., Voesenek, L. A. C. J., and van Bodegom, P. M.: Global patterns of the leaf economics spectrum in wetlands, Nat. Commun., 11, 4519, https://doi.org/10.1038/s41467-020-18354-3, 2020.
- Perri, S., Katul, G. G., and Molini, A.: Xylem-phloem hydraulic coupling explains multiple osmoregulatory responses to salt stress, New Phytologist, 224, 644–662, 2019.
- Pezeshki, S. R., DeLaune, R. D., and Patrick W. H.: Response of baldcypress (*Taxodium distichum* L. var. *Distichum*) to increases in flooding salinity in Louisiana's Mississippi River deltaic plain, Wetlands, 7, 1–10, https://link.springer.com/article/ 10.1007/BF03160798 (last access: 17 November 2025), 1987.
- Pezeshki, S. R., Pardue, J. H., and DeLaune, R. D.: Leaf gas exchange and growth of flood-tolerant and flood-sensitive tree species under low soil redox conditions, Tree Physiol, 16, 453–458, https://doi.org//10.1093/treephys/16.4.453, 1996.
- Robbins, Z., Chambers, J., Chitra-Tarak, R., Christoffersen, B., Dickman, L. T., Fisher, R., Jonko, A., Knox, R., Koven, C., Kueppers, L., and McDowell, N.: Future climate doubles the risk of hydraulic failure in a wet tropical forest, New Phytol., 244, 2239–2250, 2024.
- Rubol, S., Silver, W. L., and Bellin, A.: Hydrologic control on redox and nitrogen dynamics in a peatland soil, Science of the total environment, 432, 37–46, 2012.
- Saber, A., Cheng, V. Y., and Arhonditsis, G. B.: Evidence for increasing influence of atmospheric teleconnections on

- water levels in the Great Lakes, J. Hydrol., 616, 128655, https://doi.org/10.1016/j.jhydrol.2022.128655, 2023.
- Sairam, R. K., Kumutha, D., Ezhilmathi, K., Deshmukh, P. S., and Srivastava, G. C.: Physiology and biochemistry of waterlogging tolerance in plants, Biol. Plant., 52, 401–412, 2008.
- Sallenger, A. H., Doran, K. S., and Howd, P. A.: Hotspot of accelerated sea-level rise on the Atlantic coast of North America, Nat. Clim. Change, 2, 884–888, https://doi.org/10.1038/nclimate1597, 2012.
- Schenk, H. J. and Jackson, R. B.: The global biogeography of roots, Ecol. Monogr., 72, 311–328, 2002.
- Schieder, N. W., Walters, D. C., and Kirwan, M. L.: Massive upland to wetland conversion compensated for historical marsh loss in Chesapeake Bay, USA, Estuaries and coasts, 41, 940–951, 2018.
- Shaw, P., Jobe, J., and Gedan, K. B.: Environmental limits on the spread of invasive Phragmites australis into upland forests with marine transgression, Estuaries and Coasts, 45, 539–550, 2022.
- Sippo, J., Lovelock, C. E., Santos, I. R., Sanders, C. J., and Maher, D. T.: Mangrove mortality in a changing climate: An overview, Estuar. Coast. Shelf Sci., 215, 241–249, https://doi.org/10.1016/j.ecss.2018.10.011, 2018.
- Smith, I. M., Fiorino, G. E., Grabas, G. P., and Wilcox, D. A.: Wetland vegetation response to record-high Lake Ontario water levels, J. Great Lakes Res., 47, 160–167, 2021.
- Spalding, M. D., Ruffo, S., Lacambra, C., Meliane, I., Hale, L. Z., Shepard, C. C., and Beck, M. W.: The role of ecosystems in coastal protection: Adapting to climate change and coastal hazards, Ocean Coast. Manag., 90, 50–57, 2014.
- Sperry, J. S., Wang, Y., Wolfe, B. T., Mackay, D. S., Anderegg, W. R., McDowell, N. G., and Pockman, W. T.: Pragmatic hydraulic theory predicts stomatal responses to climatic water deficits, New Phytologist, 212, 577–589, https://doi.org/10.1111/nph.14059, 2016.
- Sperry, J. S., Adler, F. R., Campbell, G. S., and Comstock, J. P.: Limitation of plant water use by rhizosphere and xylem conductances: Results from a model, Plant Cell Environ., 21, 347–357, https://doi.org/10.1046/j.1365-3040.1998.00287.x, 1998.
- Suárez, N., and Medina, E.: Influence of salinity on Na+ and K+ accumulation, and gas exchange in Avicennia germinans, Photosynthetica, 44, 268–274, 2006.
- Sward, R., Philbrick, A., Morreale, J., Baird C. J., and Gedan K.: Shrub expansion in maritime forest responding to sea level rise, Frontiers in Forests and Global Change, 6, 11 pp., https://www.frontiersin.org/journals/forests-and-global-change/articles/10.3389/ffgc.2023.1167880/full (last access: 17 November 2025), 2023.
- Tagestad, J., Ward, N. D., Butman, D., and Stegen, J.: Small streams dominate US tidal reaches and will be disproportionately impacted by sea-level rise, Science of The Total Environment, 753, p.141944, 2021.
- Taherkhani, M., Vitousek, S., Barnard, P. L., Frazer, N., Anderson, T. R., and Fletcher, C. H.: Sea-level rise exponentially increases coastal flood frequency, Sci. Rep., 10, 1–17, 2020.
- Theuerkauf, E. J. and Braun, K. N.: Rapid water level rise drives unprecedented coastal habitat loss along the Great Lakes of North America, J. Great Lakes Res., 47, 945–954, 2021.
- Theuerkauf, E. J., Braun, K. N., Nelson, D. M., Kaplan, M., Vivirito, S., and Williams, J. D.: Coastal geomorphic response to seasonal water-level rise in the Laurentian Great Lakes: An exam-

- ple from Illinois Beach State Park, USA, J. Great Lakes Res., 45, 1055–1068, 2019.
- Thiéblemont, R., Le Cozannet, G., D'anna, M., Idier, D., Belmadani, A., Slangen, A. B., and Longueville, F.: Chronic flooding events due to sea-level rise in French Guiana, Sci. Rep., 13, 21695, https://doi.org/10.1038/s41598-023-48807-w, 2023.
- Ury, E. A., Yang, X., Wright, J. P., and Bernhardt, E. S.: Rapid deforestation of a coastal landscape driven by sealevel rise and extreme events, Ecol. Appl., 31, e02339, https://doi.org/10.1002/eap.2339, 2021.
- Varekamp, J. C., Thomas, E., and Van de Plassche, O.: Relative sea-level rise and climate change over the last 1500 years, Terra Nova, 4, 293–304, 1992.
- Wang, W., McDowell, N. G., Ward, N. D., Indivero, J., Gunn, C., and Bailey, V. L.: Constrained tree growth and gas exchange of seawater-exposed forests in the Pacific Northwest, USA, Journal of Ecology 107, 2541–2552, https://doi.org/10.1111/1365-2745.13225, 2019.
- Wang, W., Zhang, P., Zhang, H., Grossiord, C., Pennington, S. C., Norwood, M. J., Li, W., Pivovaroff, A. L., Fernández-De-Uña, L., Leff, R., Yabusaki, S. B., Waichler, S., Bailey, V. L., Ward, N. D., and McDowell, N. G.: Severe declines in hydraulic capacity and associated carbon starvation drive mortality in seawater exposed Sitka-spruce (Picea sitchensis) trees, Environmental Research Communications, 4, https://doi.org/10.1088/2515-7620/ac5f7d, 2022.
- Wilcox, D. A.: Implications of hydrologic variability on the succession of plants in Great Lakes wetlands, Aquat. Ecosyst. Health Manag., 7, 223–231, 2004.
- Wilcox, D. A. and Nichols, S. J.: The effects of water-level fluctuations on vegetation in a Lake Huron wetland, Wetlands, 28, 487–501, 2008.
- Xu, C., Christoffersen, B., Robbins, Z., Knox, R., Fisher, R. A., Chitra-Tarak, R., Slot, M., Solander, K., Kueppers, L., Koven, C., and McDowell, N.: Quantification of hydraulic trait control on plant hydrodynamics and risk of hydraulic failure within a demographic structured vegetation model in a tropical forest (FATES-HYDRO V1.0), Geosci. Model Dev., 16, 6267–6283, https://doi.org/10.5194/gmd-16-6267-2023, 2023.
- Yadav, S., Irfan, M., Ahmad, A., and Hayat, S.: Causes of salinity and plant manifestations to salt stress: a review, Journal of environmental biology, 32, 667–685, PMID 22319886, 2011.
- Zaerr, J. B.: Short-term flooding and net photosynthesis in seedlings of three conifers, Forest Science, 29, 71–78, 1983.
- Zeng, X.: Global vegetation root distribution for land modeling, J. Hydrometeorol., 2, 525–530, 2001.
- Zhang, P., McDowell, N. G., Zhou, X., Wang, W., Leff, R. T., Pivovaroff, A. L., Zhang, H., Chow, P. S., Ward, N. D., Indivero, J., and Yabusaki, S. B.: Declining carbohydrate content of Sitkaspruce trees dying from seawater exposure, Plant Physiol., 185, 1682–1696, https://doi.org/10.1093/plphys/kiab002, 2021a.
- Zhang, P., McDowell, N. G., Zhou, X., Wang, W., Leff, R. T., Pivovaroff, A. L., Zhang, H., Chow, P. S., Ward, N. D., Indivero, J., Yabusaki, S. B., Waichler, S., and Bailey V. L.: Declining carbohydrate content of Sitka-spruce treesdying from seawater exposure, Plant Physiology, 185, 1682–1696, https://doi.org/10.1093/plphys/kiab002, 2021b.
- Zhao, C., Zhang, H., Song, C., Zhu, J. K., and Shabala, S.: Mechanisms of plant responses and adaptation to soil salinity, The Inno-

- vation, 1, 100017, https://doi.org/10.1016/j.xinn.2020.100017, 2020
- Zhou, J., Zhang, J., Chen, Y., Qin, G., Cui, B., Lu, Z., Wu, J., Huang, X., Thapa, P., Li, H., and Wang, F.: Blue carbon gain by plant invasion in saltmarsh overcompensated carbon loss by land reclamation, Carbon Res., 2, 39, https://doi.org/10.1007/s44246-023-00070-4, 2023.